Assessment of multiparametric MRI in a human glioma model to monitor cytotoxic and anti-angiogenic drug effects.

Benjamin Lemasson, Thomas Christen, Xavier Tizon, Régine Farion, Nadège Fondraz, Peggy Provent, Christoph Segebarth, Emmanuel L Barbier, Philippe Genne, Olivier Duchamp, et al.

Assessment of multiparametric MRI in a human glioma model to monitor cytotoxic and antiangiogenic drug effects

LEMASSON Benjamin, Msc[1,2,3], CHRISTEN Thomas, MSc[2,3], TIZON Xavier, PhD[1], FARION Régine[2,3], FONDRAZ Nadège[2,3], PROVENT Peggy, PhD[1], SEGEBARTH Christoph, PhD[2,3], BARBIER Emmanuel L, PhD.[2,3], GENNE Philippe, PhD[1], DUCHAMP Olivier[1,†] and REMY Chantal, PhD[2,3,†,*]

[1]Oncodesign Biotechnology, Dijon, France

[2]Inserm, U836, Grenoble, F-38043, France

[3]Université Joseph Fourier, Grenoble Institut des Neurosciences, UMR-S836, Grenoble, F-38043, France

† Last two authors contributed equally to this paper.

*Corresponding author:

REMY Chantal
Grenoble Institut des Neurosciences (GIN) - INSERM U836 / Equipe 5
Neuroimagerie Fonctionnelle et Métabolique
Université Joseph Fourier - Site Santé de la Tronche
Domaine de la Merci
38042 La Tronche Cedex, France
chantal.remy@ujf-grenoble.fr
Tel: +33 4 56 52 05 89
Fax: +33 4 56 52 05 98

Running headline: Multiparametric MRI to monitor anti-tumoral drugs

Key words: Apparent diffusion coefficient of water (ADC), blood volume fraction (BVf), brain tumor, Contrast enhancement MRI, therapies, vessel size index (VSI).

Abbreviations used: ADC, Apparent Diffusion Coefficient of water; BVf, Blood Volume fraction; CE, Contrast Enhancement; VSI, Vessel Size Index; RecA-1, Rat Endothelial Cell Antigen-1;

Abstract

Early imaging or blood biomarkers of tumor response are needed to customize anti-tumor therapy, on an individual basis. This study evaluates the sensitivity and the relevance of five potential MRI biomarkers.

Sixty *Nude* rats were implanted with human glioma cells (U-87 MG) and randomized into 3 groups: one group received an anti-angiogenic treatment (Sorafenib), a second a cytotoxic drug (BCNU) and the third group no treatment. Tumor volume, apparent diffusion coefficient (ADC) of water, blood volume fraction (BVf), microvessel diameter (VSI) and vessel wall integrity (CE) were monitored before and during treatment.

Sorafenib reduced tumor contrast enhancement as early as one day after treatment onset. By four days post treatment onset, tumor BVf was reduced and tumor VSI had increased. By fourteen days after treatment onset ADC was increased and tumor growth rate was reduced. With BCNU, ADC was increased and tumor growth rate was reduced 14 days after treatment onset. Thus, estimated MRI parameters were sensitive to treatment, at different times after treatment onset and in a treatment dependent way.

This study suggests that multiparametric MR monitoring could allow the assessment of new anti-tumor drugs and the optimization of combined therapies.

Introduction

Glioblastomas are the most common subtypes of rapidly growing primary brain tumors in adults. Being among the most angiogenic human tumors, they are characterized by remarkable proliferative vascular components and are often necrotic and invasive (1). Their aggressiveness is mainly due to their ability to stimulate the formation of new blood vessels (2).

Despite active efforts in therapeutics such as surgery, radiotherapy and chemotherapy, gliomas patients still have a poor prognosis and a high recurrence rate. Since 1980, the median survival of patients with glioblastoma has not increased and remains around 11 months after diagnosis (3). The lack of efficiency in conventional therapeutic approaches is related to drug delivery challenges inherent to chemoresistance. New therapeutic strategies directed against tumor vasculature or preventing angiogenesis have been developed with exciting preliminary results (4,5). Antiangiogenic drugs are likely to play a key role in the treatment of malignant glioma, mostly in association with other molecularly targeted compounds or with cytotoxic molecules (3,6).

In the clinic, the current standard for assessing the efficacy of an anti-tumor therapy is the “Response Evaluation Criteria in Solid Tumor” (RECIST) which is mainly based on measuring tumor volume from radiographic images (7). Given the observed delay between treatment onset and its effect on tumor size (several weeks or months), an early biomarker of response to therapy would allow rapid treatment adaptation or guide treatment combination, on an individual basis. These biomarkers can arise from biochemical assays (e.g. tissular or circulant markers) or from imaging modalities (8,9).

Among all imaging modalities, magnetic resonance imaging (MRI) appears as a good candidate for monitoring the effect of anti-tumor therapy. MRI is routinely used to estimate tumor volume using anatomical images, but also tumor associated edema and tumor cellularity, using the apparent diffusion coefficient (ADC) of water (10-12). Moreover, numerous microvascular parameters that appear well-suited to assess the effect of antiangiogenic drugs can be estimated using MRI, such as blood volume, blood flow, microvessel diameter, or vessel wall permeability (13-15). A recent example shows that the extent of vascular normalization measured by MRI would be predictive of the outcome of anti-Vascular Endothelial Growth Factor (anti-VEGF) therapy in glioblastomas (16).

Several studies have monitored one or two of these parameters to follow the effect of an anti-tumor therapy in addition to RECIST (17-19). Very few therapeutic follow-ups have used an MRI protocol combining more than three parameters (20). The aim of this study was to analyze various MR parameters into one protocol to assess the impact of 2 different treatments on glioma model and to evaluate whether these parameters are relevant, i.e. sensitive to a given treatment.

To address this issue, we used a combined MRI / histology protocol to monitor the effect of a cytotoxic therapy (Carmustin / BCNU; an alkylating agent) and of an antiangiogenic therapy (Sorafenib; Nexavar®; a multikinase inhibitor) a glioma model obtained by orthotopically xenografting a human glioblastoma cell line (U-87 MG) in *Nude* rats. BCNU has been chosen because it is one of the standards of care for gliomas. Sorafenib is considered as an antiangiogenic molecule and has been found efficient for several solid tumors (21). Regarding brain tumors, it was shown that Sorafenib induces growth arrest on a medulloblastoma (22) and a human glioblatoma (23) xenografted grafted in mice. Vascular effects were detected in the last case (23).

Before and three time points after treatment onset, the following MRI parameters were estimated: tumor volume, water ADC, blood volume fraction (BVf), vessel diameter (vessel size index, VSI), and vessel wall integrity (contrast enhancement, CE). The effect of treatments on each of these MRI parameters was assessed and compared to cellular and vascular characteristics described by immunohistochemistry.

Material and methods

Glioma cell line and anti-tumor drugs

The U-87 MG human glioblastoma cell line was purchased from the American Type Culture Collection (Manassas, VA). Cells were cultured in RPMI1640 medium containing 10% fetal calf serum and 2 mM glutamine.

Sorafenib (Nexavar®) was purchased from Bayer Corporation (West Haven, CT, U.S.A) and prepared as a suspension in a mixture of 5% dimethyl sulfoxide (DMSO), 5% tween-20 and 90% NaCl 0.9%.

Carmustine (1,3-bis(2-chloroethyl)-1-nitroso-urea, BCNU) was purchased from Sigma-Aldrich (St. Louis, MO, USA) and dissolved in NaCl 0.9% containing 30% of ethanol.

In vivo intracerebral U-87 MG glioma model and treatments

This study was approved by the local committee for animal care and use (approval 081). Experiments were performed under permits n° A380521, A3851610004 and B3851610003 from the French Ministry of Agriculture. Experimental design of this study is presented in figure 1a.

Male RH-*rnu/rnu Nude* rats (n=60, weight: 180-220g, Harlan Sprague Dawley, Indianapolis, USA) were prepared for xenograft by whole body irradiation with a ^{60}Co γ-source (7 Gy), 24-48 h prior to human tumor cell inoculation. Animals were

anesthetized with an intraperitoneal injection of Ketamine (75 mg/kg, Ketamine500®, Centravet, France) and Xylazine (5 mg/kg, Rompun®, Centravet, France) in 0.9% NaCl solution and immobilized in a stereotactic frame (David Kopf Instrument, Germany). Five µl of U-87 MG cell suspension in serum-free RPMI1640 medium containing 10^5 tumor cells were inoculated in the right caudate nucleus of the rat brain by stereotactic injection through a 1-mm burr hole at 2.5 mm lateral to the bregma and at a depth of 4.5 mm from the dura. The injection was performed slowly over 15 minutes, and the needle was withdrawn over another 5 minutes. The burr hole was filled with bone wax to prevent extracranial extension of the tumor.

Eleven days after tumor implantation (D11), anatomical imaging (T_2-weighted anatomical images) was performed to evaluate the volume of each tumor. Rats were then randomized and stratified in 3 groups (n=20 per group) with the similar average tumor volume per group (mean tumor volume across all rats at D11, 3.8 ± 2.2 mm^3). Treatment began 14 days after tumor implantation (Fig. 1a; $D14_{(T0)}$):

- BCNU group received two intravenous injections of BCNU (10 $mg.kg^{-1}$) on the day of treatment onset and 13 days after ($D14_{(T0)}$ and $D27_{(T13)}$).
- SORA group received daily oral administration of Sorafenib (100 $mg.kg^{-1}$) between treatment onset and the 14th day after treatment start ($D14_{(T0)}$ to $D28_{(T14)}$).
- Untreated group received no treatment.

***In vivo* MRI experiments for tumor follow-up**

Experiments were performed on a horizontal 2.35 Tesla (40 cm diameter) magnet equipped with actively shielded gradient coils (Magnex Scientific Ltd., Oxford, UK) and interfaced to a SMIS console (SMIS Ltd, Guildford, UK). MR acquisitions were performed under anesthesia: 5% isoflurane for induction and 2% for maintenance in 70% air / 30% oxygen. Rectal temperature was maintained at

37.0 ± 0.5°C throughout the experiments. After anesthesia, a catheter was inserted into the tail vein allowing injection of contrast agent without removing the rat from the magnet.

Tumor volume, ADC, BVf, VSI and CE were mapped in the tumor and contralateral hemisphere one day before and 1, 4 and 14 days after treatment onset (Fig. 1; $D13_{(T-1)}$, $D15_{(T1)}$, $D18_{(T4)}$ and $D28_{(T14)}$, respectively). The last time point was chosen to correspond to 3 days before the median survival time of untreated *Nude* rats bearing U-87 MG glioblastoma (31 days; based on the survival study – see Fig. 2a). The total duration of one MRI session was 1h30 per animal. MRI sequences were realized in the following order (Fig. 1b):

- Anatomical T_2-weighted images were acquired using a spin-echo MRI sequence (TR/TE = 2000/80 ms, 19 slices with FOV = 30x30 mm^2, matrix = 256x256 and voxel size = 117x117x1000 μm^3). Imaging time was 4 min and 17 s.
- ADC was computed from 3 diffusion weighted spin-echo images (in X, Y, and Z directions) with b = 900 $s.mm^{-2}$ and a reference image (b ≈ 0 $s.mm^{-2}$) (TR/TE = 2000/80 ms, 7 slices with FOV = 30x30 mm^2, matrix = 128x128 and voxel size = 234x234x1000 μm^3). Imaging time was 17 min.
- BVf and VSI were estimated using a multi gradient echo and spin-echo MRI sequence (MGESE) (TR = 6 s, 7 evenly spaced gradient-echoes = [6-42] ms, 1 spin-echo = 102 ms, FOV = 30x30 mm^2, matrix 128x128 and voxel size = 234x234x1000 μm^3). Imaging time was 13 min and 40 s. MGESE sequences were acquired prior to and 3 min after administration of ultra small superparamagnetic iron oxide (USPIO) via the catheter within about 20 sec (200 µmoles of iron/kg body weight; flush with 200µL of saline) (Sinerem®, Guerbet, Roissy, France; Combidex®, AMAG Pharmaceuticals, Inc, MA, USA). Sinerem® is a dextran-coated iron-based

contrast agent of about 20 nm in size and 4.5 hours plasmatic half-life in rats at this dose. The relaxivities of Sinerem® in water at 2.35T and 37°C are 8 and 89 $s^{-1}.mM^{-1}$ for r_1 and r_2 respectively (data provided by Guerbet).

- CE was assessed using T_1-weighted anatomical images acquired using a 3D-MDEFT sequence (TI = 605 ms, alpha = 22°, TR/TE = 15/5 ms, FOV 40x40x30 mm^3, matrix = 128x128x96 and voxel size = 313x313x313 μm^3). Imaging time was 4 min and 15 s. To limit the duration of the MR session per animal, a simple subtraction approach was preferred to a dynamic contrast enhanced MRI approach. Thus, one 3D-MDEFT sequence was performed before and 3 min after administration of P846 via the catheter in about 20 sec (50 µmoles/kg body weight; flush with 200µL of saline). P846 (Guerbet, Roissy, France) is a Gd-based contrast agent with a molecular weight of 3.5 kDa and a plasmatic half-life in rats of 51.1 ± 1.1 min at the concentration used (data provided by Guerbet). The relaxivities of P846, measured in water at 2.35T and 37°C are 28 and 39 $s^{-1}.mM^{-1}$ for r_1 and r_2 respectively (data provided by Guerbet). In this study we used high molecular weight contrast agent (P846: 3.5 kD), instead of a routinely used clinical agent (Gd-DOTA or Gd-DTPA: around 0.5 kD), to increase CE sensitivity to different vessel maturity (24).

For each group, 4 rats, called the “longitudinal” subgroup were imaged at each time point ($D13_{(T-1)}$, $D15_{(T1)}$, $D18_{(T4)}$ and $D28_{(T14)}$). After the last MRI measurement, animals were euthanized for subsequent *ex vivo* experiments. Per group, the sixteen remaining rats were imaged once and then euthanized at the end of imaging session to enable *ex-vivo* studies (4 animals/time point/group). They form the “single-time” subgroup (Fig. 1a). Due to experimental and technical problems (death of animals due to anesthesia, data unusable because of problems during acquisitions) only 7 out of 8 rats per group yielded acceptable data at $D13_{(T-1)}$, $D15_{(T1)}$, and $D18_{(T4)}$ and

only 4 out of 8 rats per group at $D28_{(T14)}$. Details of data usable per group (untreated, BCNU and SORA) and subgroup (single-time and longitudinal) are presented in table 1.

***Ex vivo* experiments**

At the end of the MRI experiment, the animals were humanely sacrified (Fig. 1a). The brain was quickly removed, frozen in -40°C isopentane and stored at -80°C until processing. Brains were sliced at -20°C with a cryostat (10 µm thick sections).

First, anatomic changes associated with BCNU and Sorafenib treatment were analyzed using hematoxylin and eosin (HE) staining.

Secondly, vascular components were analyzed by immunohistochemistry of the vessel basal lamina with collagen IV labeling and of endothelial cells using rat endothelial cell antigen-1 labeling (RecA-1). These two stainings assess the impact of anti-tumor treatments on vessel integrity. Slices were rehydrated in phosphate-buffered saline (PBS, 0.01M) and fixed in 4% paraformaldehyde. After saturation in PBS-Tween 0.01%-BSA 3% for 30 min at room temperature, primary antibodies (a goat antibody against collagen IV, Southern Biotech, ref 1340-01, 1/2000; a mouse antibody against RecA-1, AbD Serotec ref. MCA9070R, 1/200) were incubated overnight at 4°C in PBS-Tween 0.01%-BSA 1%. Secondary antibodies were Alexa 546-linked Donkey anti-goat IgG (Invitrogen, A11030, 1/200) and Alexa 488 linked Donkey anti-mouse IgG (Invitrogen, A21202, 1/200).

Survival Study

The effects of both treatments on the mean survival of *Nude* rats bearing a human glioblastoma xenografts were assessed on 6 additional rats per group (untreated, BCNU, and SORA groups) implanted and treated as described above.

Animals were sacrificed at the onset of neurological signs (according to Redgate et al. (25)). Increased lifespan (ILS) was estimated for each treated group compared (in percent). ILS was calculated using the mean survival time (MST) of each group as following: ILS (%) = ($MST_{untreated}$ – $MST_{treated}$)/ $MST_{untreated}$

Control MRI experiment: evaluation of USPIO extravasation

The MR method used to estimate BVf and VSI uses as a starting hypothesis that the contrast agent remains intravascular (26). To estimate the amount of USPIO that extravasates during BVf and VSI measurements, dynamic contrast-enhanced MRI (DCE-MRI: T_1-based) was performed on another set of tumor bearing rats (n=12, in addition to those already mentioned). For this 'control' experiment, we used a dedicated MRI protocol (Fig. 1c). At each time point, the 4 animals of each group (SORA, BCNU and untreated groups) were imaged with multiple T_{1w} spin-echo images (TR/TE = 600/17ms, 11 slices with FOV = 30x30 mm^2, matrix 128x128 and voxel size = 234x234x1000 μm^3, 1 min 17 s/image; 17 repetitions; total acquisition time = 21 min 49s). After one repetition (i.e. 1 min 17s after imaging start), Sinerem® was administered via the catheter in about 20 sec (200 µmoles of iron/kg body weight; flush with 200 µL of saline).

Data analysis

Determination of tumor volume (Fig. 1b): Tumor volume was obtained by manually delineating the tumors on anatomical T_2-weighted MR images from adjacent slices containing the lesions, counting voxels within the tumor boundaries, and scaling with the voxel volume.

ADC, BVf and VSI (Fig. 1b): Data were processed as described in Valable et al. (26) using in-house developed software in the Matlab® environment. To avoid partial volume effects that occur in slices located on the edge of the tumor (healthy and

tumoral tissue are mixed), regions of interest (ROIs) were manually delineated over the tumor on the 3 T_2-weighted slices containing the largest tumor area. Contralateral ROIs were defined in the contralateral striatum on the same slices. ROIs were transferred to ADC, BVf and VSI maps. Then, within each ROI and each map, voxels for which the analysis could not be performed were identified (e.g. voxels with non-converging fit and voxels with values outside the range of validity of the method (ADC>3500 $\mu m^2.s^{-1}$; BVf>17%, VSI>50 µm) and excluded from the analysis. The total number of voxels, the number of excluded voxels, and the mean and standard deviation over the 3 analyzed slices for a rat were computed for each ROI and each parameter. Rejected voxels per ROI represented 4.5% for tumor and 0.5% contralateral striatum of the total number of voxels, for all groups.

CE: Vessel integrity was assessed using the T_{1w} images acquired before ($T_{1w(before)}$) and 3 min after ($T_{1w(after)}$) injection of P846 as describe by equation 1. The mean and standard deviation were computed for each group using the same ROI described above.

$$CE = \frac{SI(T_{1w(after)}) - SI(T_{1w(before)})}{SI(T_{1w(before)})} \qquad \text{equation 1}$$

SI : Signal Intensity

USPIO extravasation (Fig. 1c): Since DCE-MRI images were acquired with a TE = 17 ms, a decrease in signal (due to T_2^* reduction, intravascular USPIO) was observed just after injection of USPIO, after which, in case of extravasation, signal increased (T_1 reduction, extravascular USPIO). The relative increase in signal between the first image acquired after USPIO injection and the last image of the DCE-MRI protocol was assigned to T_1 effect. Eventually, this signal enhancement was converted to extravascular iron concentration as described by Valable et al. (26). Since we neglected the plasmatic clearance of USPIO in our analysis, we

overestimated the T_1 effects and thus obtained an upper limit of the extravascular iron concentration.

Quantitative histology: Sections corresponding to MRI images (up to three microscopic fields per ROI and animal) were digitized using a CCD camera (Olympus, Rungis, France). Collagen IV images were thresholded and vascular parameters (mean vessel density, fractional vascular surface area, mean vessel radius) were obtained using ImageJ software (Rasband,W.S., ImageJ) as described by Valable et al. (26). The number of vessels stained by Collagen IV and RecA has been account manually onto the immunohistologies images and then the percentage of vessels doubly stained was calculated. We also realized a manual quantification of the cell density from the HE sections (cells/mm^2).

Statistical analysis

Paired t tests were used for comparing tumor versus contralateral striatum inside the same group. Comparisons between each group were subjected to factorial analysis of variance with a Protected Least Significant Difference (PLSD) Fisher's test as post hoc test (intergroup analysis). $p<0.05$: *; $p<0.01$: ** and $p<0.001$: ***. Survival was visualized using Kaplan-Meier curves and differences between groups assessed with a log-rank test. All statistics were performed with SPSS (SPSS Inc, Chicago, Ill, USA). Results are presented as mean ± standard deviation and are given by group, by time point and by region of interest.

Results

Accuracy of the BVf and VSI measurements

Using our model, accurate BVf and VSI measurements require that the iron-based contrast agent remains intravascular. At each time point, USPIO extravasation data were not statistically different across all groups (data were thus pooled). In contralateral tissue, iron concentration remained below the detection sensitivity of our DCE-MRI approach (≤1μM) (26). Nineteen minutes after USPIO injection (corresponding to the end of MR data acquisition in BVf/VSI measurement), the average iron concentration in the tumor across all groups and time points was 2.6 ± 0.4 μM. This concentration corresponds to 0.3% of the plasma iron concentration (3420 ± 970 μM, data reported by Valable et al. (26)).

Longitudinal MRI follow-up

In a longitudinal study, repeated anesthesia and contrast agent injections might affect the physiological status of the animal, the rate of tumor growth and the accuracy of the MRI measurements. To check this, we compared for each group the "single-time" and the "longitudinal" subgroups at each time point and we observed no difference in body weight, tumor size, ADC, BVf, VSI and in CE between. In this experiment, a longitudinal study (repetition of MRI protocol) has no effect on the assessed parameters. Consequently, for the 3 groups, values from the “single-time” and “longitudinal” subgroups were pooled at each time-point.

In vivo anti-tumor activity of BCNU and Sorafenib treatments

MRI data in contralateral rat brain hemisphere

No significant difference over time and across the 3 groups in ADC, BVf and VSI was detected contralaterally (720±85 $\mu m^2.s^{-1}$, 3.3±0.5% and 5.6±1.1µm for ADC, BVf and VSI mean across time points and groups respectively). Consequently, the mean contralateral value across groups is represented at each time point, for the sake of clarity (Fig. 3; dotted line). However, intragroup comparisons between tumor and contralateral tissues were performed using the contralateral values of each group.

U-87 MG tumor development (untreated group)

Median survival time of untreated U-87 MG glioblastoma cells bearing Nude rats was 31 days (Fig. 2a). The volume of the untreated U-87 MG tumors increased rapidly between $D13_{(T-1)}$ and $D28_{(T14)}$ (4.5 ±1.4 to 117.1 ± 22.9 mm^3 respectively; Fig. 2b). ADC, BVf and VSI in U-87 MG tumors were significantly higher than in the contralateral striatum and remained stable with time (tumor: 851 ± 43 $\mu m^2.s^{-1}$, 4.4 ± 0.3 % and 7.9 ± 1.2 µm; contralateral striatum: 720 ± 85 $\mu m^2.s^{-1}$, 3.3 ± 0.5 % and 5.5 ± 0.3 µm for ADC, BVf and VSI respectively, mean value across the four time points, $p<0.001$; Fig. 3a-c). In the untreated group, glioma vessels were permeable to P846 during follow-up (CE: 190 ± 47 %, mean across all time points; Fig. 3d).

Effect of BCNU on U-87 MG glioma (BCNU group)

BCNU treatment slightly increased (but not significantly) the median survival of U-87 MG glioma bearing rats (+16%; Fig. 2a). BCNU treatment strongly inhibited tumor growth compared to untreated group (5.7 ± 4.9 vs. 117.1 ± 22.9 mm^3, for the BCNU and untreated groups respectively, at $D28_{(T14)}$, $p<0.001$; Fig. 2b). Intratumoral ADC was comparable between the BCNU and untreated groups at all time points except at $D28_{(T14)}$ when ADC in the BCNU group became significantly larger than in the untreated group (1048 ± 10 vs. 794 ± 49 $\mu m^2.s^{-1}$, $p<0.001$; Fig. 3a). VSI, BVf and

CE in the BCNU group did not differ from those measured in the untreated group (Figs. 3b-d).

Effect of Sorafenib on U-87 MG glioma (SORA group)

Sorafenib treatment induced a small increase (but not significantly) of the median survival time of the U87-MG glioma bearing rats as compared to the untreated group (+23%; Fig. 2a). Sorafenib treatment significantly inhibited tumor growth as compared to untreated group (28.7 ± 11.1 vs. 117.1 ± 22.9 mm^3, respectively, at $D28_{(T14)}$, $p<0.001$; Fig. 2b). We also observe, at $D28_{(T14)}$, that the tumoral volume into the SORA group were statistically greater than that of the BCNU group (28.7 ± 11.1 vs. 5.7 ± 4.9 mm^3, respectively, at $D28_{(T14)}$, $p<0.001$; Fig. 2b). At $D28_{(T14)}$, ADC in the SORA group was larger than in the untreated group (976 ± 37 and 794 ± 49 $\mu m^2.s^{-1}$, respectively, $p<0.01$; Fig. 3a).

All vascular parameters assessed in this study (VSI, BVf and CE) were modified by Sorafenib. While tumoral VSI in the SORA and untreated groups were similar before treatment ($D13_{(T-1)}$), tumoral VSI in the SORA group became significantly larger than in the untreated group as early as $D18_{(T4)}$ and up to $D28_{(T14)}$ ($D18_{(T4)}$: 7.2 ± 1.8 vs 5.8 ± 1.8 µm; $p<0.001$ and $D28_{(T14)}$: 12.4 ± 1.7 vs 8.7 ± 1.7 µm; $p<0.01$, respectively; Fig 3b). In the SORA group, the tumoral BVf decreased from treatment onset ($D15_{(T1)}$: 5.0 ± 0.8 to $D28_{(T14)}$: 2.6 ± 1 %; Fig. 3c) while it remained stable in the untreated group ($D15_{(T1)}$: 5.2 ± 0.9 to $D28_{(T14)}$: 5.5 ± 0.8 %; Fig. 3c). In contrast to what happens in untreated and BCNU group, in the SORA group the extravasation of P846 was significantly reduced as early as 1 day after Sorafenib treatment start (CE: 116 ± 65% vs 184 ± 42% for the SORA and untreated groups respectively at $D15_{(T1)}$) and was not detectable at $D28_{(T14)}$ (Fig. 3d).

HE staining

From $D13_{(T-1)}$ to $D18_{(T4)}$, U-87 MG tumors in the untreated, BCNU and SORA groups presented very similar anatomical histological structures on HE stained sections. Cell density was higher in the tumor core with some tumor cells aligned along vessels, forming thin bundles. Tumors were surrounded by a ring of highly edematous tissue. Neither necrosis nor pseudo-cyst was observed (Fig. 4a). At $D28_{(T14)}$, in the SORA and BCNU groups tumor cell density was reduced compared to previous time points and edematous areas appeared inside the tumor tissue (Fig. 4a).

Vascular staining

To assess variation in vasculature properties, collagen IV and RecA labelings were performed (Fig. 4). For all groups and all time points, vessels in contralateral striatum exhibited similar diameter, density and vascular surface area (4.4 ± 0.2 µm, 337 ± 37 vessels per mm^2 and 3.76 ± 0.34 % vascular surface area; mean across all groups and all time points; Fig. 4b-d). All vessels were also stained by Collagen IV and RecA (Fig. 4a). Before treatments, in all groups, tumor vessel diameters were larger than in the contralateral striatum (5.2 ± 0.6; 5.4 ± 0.6 and 6 ± 0.3 µm versus 4.2 ± 0.2 µm for untreated, BCNU and SORA groups versus mean of contralateral striatum across all group, respectively; $p<0.05$; Fig. 4b) and vascular surface area was higher than in contralateral striatum (9.1 ± 1.4; 6.2 ± 1.3 and 7.7 ± 0.3 % versus 3.7 ± 0.5 % for untreated, BCNU and SORA groups versus mean of contralateral striatum across all group, respectively; $p<0.05$; Fig. 4c). Vascular parameters were stable with time in the untreated and BCNU groups (Fig. 4b-d).

At $D28_{(T14)}$, in the SORA group, tumor vessel density was lower compared to untreated group (141 ± 21 versus 301 ± 60 vessels per mm^2 respectively; $p<0.01$) and vascular area was similar to that in contralateral striatum (3.7 ± 1.4 versus

3.7 ± 0.3 %, respectively; p = 0.45; Fig. 4c), but vessel diameter was higher than in contralateral striatum (5.8 ± 0.7 versus 4.2 ± 0.1 vessels per mm², respectively; p<0.05; Fig. 4b). Finally, only a fraction (63 %; Fig. 4a) of the tumor vessels stained by Collagen IV antibody was also stained by RecA antibody in SORA group as compared to untreated and BCNU groups (100 %; Fig. 4a).

Discussion

The effect of two different treatments (BCNU, an alkylating agent and Sorafenib, a multikinase inhibitor) on an orthotopic human glioblastoma xenografted in *Nude* rats (U-87 MG cell line) was investigated by MRI and by immunohistology. MRI highlighted an important inhibition of tumor growth induced by both Sorafenib and BCNU treatments. As previously demonstrated, ADC, BVf and VSI values were higher in the tumor tissue than in the contralateral striatum. Sorafenib treatment induced significant differences first on tumor contrast enhancement ($D13_{(T-1)}$), then on BVf and VSI ($D18_{(T4)}$), and finally on ADC and tumor size ($D28_{(T14)}$) compared to control animals. In the BCNU group, only tumor size and ADC were modified 14 days after treatment onset.

As a first prerequisite of this study, we determined whether our extensive MR protocol could be repeated to monitor therapy response on brain tumor. First, we compared for each group the “single-time” and the “longitudinal” subgroups. In each “longitudinal” subgroup repeated anesthesia, repeated injection of contrast agent, and treatment (BCNU or Sorafenib) had no detectable effect on body weight (data not shown), tumor volume, or on MR-determined parameters as compared to the “single-time” subgroup. The second prerequisite was to assess whether the USPIO extravasated in this tumor model within the time frame of the MR session. A separate experiment, performed on 4 animals per group followed at each time point ($D13_{(T-1)}$, $D15_{(T1)}$, $D18_{(T4)}$ and $D28_{(T14)}$), showed that the extravascular concentration of USPIO in the tumor was at most 0.3% of the plasmatic concentration 20 min after injection. This result validates the main hypothesis of the VSI and BVf measure, considering the USPIO as an intravascular contrast agent. Moreover, it showed that the complete imaging protocol could fit within approximatively 90 minutes, which allows designing

follow-up experiments with a sufficient number of animals per group. All these results indicate that our experimental protocol was appropriate to monitor the effect of anti-tumoral therapies in our U-87 MG tumor model.

The goal of this study was to assess the sensitivity of multiparametric MRI to monitor the anti-tumor activity of BCNU and Sorafenib.

ADC in tumor was increased by both treatments compared to the untreated group 14 days after treatment onset thus showing the slowest evolution under both treatments. This increase is consistent with the cytotoxic effect of BCNU, and the ADC is also known to be affected by changes in cell density (or cellularity) (27) and by the occurrence of vasogenic edema. HE staining showed that cell density was smaller in the tumors of treated groups than in the untreated group 14 days after treatment onset. HE staining also showed intratumoral edema in treated groups. Even if the mechanisms involved in ADC changes are complex, these histological findings could explain the increase in intratumoral ADC in BCNU and SORA groups observed 14 days after treatment onset.

Tumor microvasculature properties assessed by both MRI and histology were not changed by the BCNU treatment. Conversely, Sorafenib induced significant modifications in tumor microvasculature. Four days after antiangiogenic treatment onset, the mean intratumoral BVf was markedly reduced compared to the untreated group and was close to its normal value. This result suggests a tendency towards normalization of tumor vasculature: under antiangiogenic treatment, the tumor vasculature becomes more similar to healthy tissue. However, at the same time point ($D18_{(T4)}$), tumoral VSI was increased by Sorafenib, with values higher than that observed in animals of untreated group. The quantitative immunohistochemistry of

tumor vessels confirmed these observations on vessel diameters and also indicated that the vessel density had decreased, as found by Siegelin et al. (23). The decrease in vessel density observed in immunohistochemistry images is consistent with the decrease in BVf and the concomitant increase in vessel diameter observed by MRI. In addition to these morphological changes, 1 day after the start of Sorafenib treatment ($D15_{(T1)}$), immunohistochemistry showed some collagen IV-positive vessels without RecA labeling. These observations indicate that some tumor vessels were formed only with basal lamina. This discrepancy between both labelings was even more pronounced after 4 and 14 days of treatment. This has been previously reported in several studies (28,29). Inai et al. observed collagen IV-positive vessels without endothelial marker in spontaneous pancreatic islet tumors treated with a VEGFRs inhibitor.

We also observed a decrease in tumor contrast enhancement as soon as 1 day after antiangiogenic treatment onset. This reduction was more pronounced 4 days after treatment onset and no P846 contrast agent extravasation was detectable 14 days after treatment onset. BVf and VSI estimates using an intravascular contrast agent (USPIO) injection show perfusion from at least a fraction of tumoral vessels under antiangiogenic treatment. These different BBB permeabilities between contrast agents with different sizes have already been described in the study by Turetschek et al. (30). Together these results could indicate that the absence of contrast enhancement of tumors after 14 days of Sorafenib treatment is due to modifications of vessel permeability and not due to a lack of tumor perfusion. Modifications of vessel integrity observed in our study are consistent with results of Flaherty et al. who observed, by MRI, a decrease in vessel permeability/perfusion (K_{trans}) after 3-12 weeks of Sorafenib treatment in patients bearing a renal cell carcinoma (17).

In our study, BVf and CE parameters indicated a normalization of tumoral vessels under antiangiogenic treatment, which has already been described in several studies (20,31). In addition to these two MR parameters, estimates of VSI indicate that tumor vessels had abnormal size compared to vessels in healthy tissue. A normalization of vascular permeability/perfusion associated to an increase in vessel diameters under antiangiogenic treatment has already been described (32). These results highlight the necessity to measure VSI, BVf and CE parameters together to monitor the different aspects of tumor microvasculature under antiangiogenic treatment. An important step in future studies will be to demonstrate that all the MR parameters used to evaluate the impact of anti-tumoral treatments are independent of each other. After this demonstration we could relate, using multivariate statistical methods, MR parameters with animal survival or tumor progression as proposed by Sorensen et al. with 2 MR parameters plus one biological measurement associated with patient outcome (16).

Glioblastomas are tumors that are highly resistant to many types of treatment. Monotherapies with antiangiogenic or cytotoxic drugs, like Sorafenib or BCNU respectively, demonstrated moderate efficacy in the U-87 MG glioblatoma. However, despite their low effectiveness on the overall survival of animals, MRI biomarkers reveal that drugs effectively reach their target and eventually induce both morphological and physiological changes for which drugs were designed. This could be helpful for pharmacological treatment optimization or combination.

The multiparametric MRI approach described in this study allowed the measurement of various characteristics of cellular and vascular remodeling that occurs due to therapy. To further complete this characterization, additional MRI developments can be foreseen or refined analysis could be evaluated. In our study

we use a CE-MRI method to evaluate vessel wall integrity. However, this parameter depends on blood flow, vessel wall permeability and diffusion of contrast agent into the extravascular compartment. An appropriate data model (33,34) could be used to quantify the change in vascular permeability and in blood flow. This requires a protocol optimization to allow measurements of VSI, BVf (using USPIO) and permeability/perfusion (using Gd-based contrast agent) in the same MRI session (35). Blood flow could also be obtained using Dynamic Susceptibility Contrast MRI or Arterial Spin Labeling (36). Using a quantitative analysis of T_2* decay (37), one could estimate the oxygen extraction fraction in the tumor, a possible marker of tumor hypoxia.

In conclusion, this study indicates that numerous changes occur in the tumor microvasculature and cellularity after antiangiogenic or cytotoxic therapy. This study also indicates that the sensitivity of the studied MR parameters varies for a given treatment and is also treatment dependent. Moreover, these changes appear complex and may not be summarized by a single physiological measurement. MRI appears as an imaging modality that can follow, non-invasively, several microvascular and cellular parameters with a strong potential for the evaluation of new drugs on brain tumors. In addition, these parameters could provide methods to better describe and understand the mechanisms of action of antiangiogenic or antivascular therapies, allowing the rational design of optimized combinations with chemotherapy and/or radiotherapy.

Acknowledgements

B.L. benefited from a doctoral grant from ‘Agence national de la Recherche et de la technologie’. We thank Guerbet for providing Sinerem® and P846, the ‘Institut National du Cancer’, the ‘Région Rhône-Alpes’ and the ‘Cancéropôle Lyon Auvergne Rhône-Alpes’ for financial support.

References

1. Jain RK, di Tomaso E, Duda DG, Loeffler JS, Sorensen AG, Batchelor TT. Angiogenesis in brain tumours. Nat Rev Neurosci 2007;8(8):610-622.
2. Folkman J. Role of angiogenesis in tumor growth and metastasis. Semin Oncol 2002;29(6 Suppl 16):15-18.
3. Burnet NG, Lynch AG, Jefferies SJ, Price SJ, Jones PH, Antoun NM, Xuereb JH, Pohl U. High grade glioma: imaging combined with pathological grade defines management and predicts prognosis. Radiother Oncol 2007;85(3):371-378.
4. Tabatabai G, Stupp R. Primetime for antiangiogenic therapy. Curr Opin Neurol 2009.
5. Dietrich J, Norden AD, Wen PY. Emerging antiangiogenic treatments for gliomas - efficacy and safety issues. Curr Opin Neurol 2008;21(6):736-744.
6. Nghiemphu PL, Liu W, Lee Y, Than T, Graham C, Lai A, Green RM, Pope WB, Liau LM, Mischel PS, Nelson SF, Elashoff R, Cloughesy TF. Bevacizumab and chemotherapy for recurrent glioblastoma: a single-institution experience. Neurology 2009;72(14):1217-1222.
7. Husband JE, Schwartz LH, Spencer J, Ollivier L, King DM, Johnson R, Reznek R, Society ICI. Evaluation of the response to treatment of solid tumours - a consensus statement of the International Cancer Imaging Society. Br J Cancer 2004;90(12):2256-2260.
8. Gagner J-P, Law M, Fischer I, Newcomb EW, Zagzag D. Angiogenesis in gliomas: imaging and experimental therapeutics. Brain Pathol 2005;15(4):342-363.

9. Jain RK, Duda DG, Willett CG, Sahani DV, Zhu AX, Loeffler JS, Batchelor TT, Sorensen AG. Biomarkers of response and resistance to antiangiogenic therapy. Nat Rev Clin Oncol 2009;6(6):327-338.

10. Hamstra DA, Chenevert TL, Moffat BA, Johnson TD, Meyer CR, Mukherji SK, Quint DJ, Gebarski SS, Fan X, Tsien CI, Lawrence TS, Junck L, Rehemtulla A, Ross BD. Evaluation of the functional diffusion map as an early biomarker of time-to-progression and overall survival in high-grade glioma. Proc Natl Acad Sci U S A 2005;102(46):16759-16764.

11. Ross BD, Moffat BA, Lawrence TS, Mukherji SK, Gebarski SS, Quint DJ, Johnson TD, Junck L, Robertson PL, Muraszko KM, Dong Q, Meyer CR, Bland PH, McConville P, Geng H, Rehemtulla A, Chenevert TL. Evaluation of cancer therapy using diffusion magnetic resonance imaging. Mol Cancer Ther 2003;2(6):581-587.

12. Cha S. Neuroimaging in neuro-oncology. Neurotherapeutics 2009;6(3):465-477.

13. Barrett T, Brechbiel M, Bernardo M, Choyke PL. MRI of tumor angiogenesis. J Magn Reson Imaging 2007;26(2):235-249.

14. Pike MM, Stoops CN, Langford CP, Akella NS, Nabors LB, Gillespie GY. High-resolution longitudinal assessment of flow and permeability in mouse glioma vasculature: Sequential small molecule and SPIO dynamic contrast agent MRI. Magn Reson Med 2009;61(3):615-625.

15. Beaumont M, Lemasson B, Farion R, Segebarth C, Rémy C, Barbier EL. Characterization of tumor angiogenesis in rat brain using iron-based vessel size index MRI in combination with gadolinium-based dynamic contrast-enhanced MRI. J Cereb Blood Flow Metab 2009.

16. Sorensen AG, Batchelor TT, Zhang W-T, Chen P-J, Yeo P, Wang M, Jennings D, Wen PY, Lahdenranta J, Ancukiewicz M, di Tomaso E, Duda DG, Jain RK. A "vascular normalization index" as potential mechanistic biomarker to predict survival after a single dose of cediranib in recurrent glioblastoma patients. Cancer Res 2009;69(13):5296-5300.

17. Flaherty KT, Rosen MA, Heitjan DF, Gallagher ML, Schwartz B, Schnall MD, O'Dwyer PJ. Pilot study of DCE-MRI to predict progression-free survival with sorafenib therapy in renal cell carcinoma. Cancer Biol Ther 2008;7(4):496-501.

18. Zwick S, Strecker R, Kiselev V, Gall P, Huppert J, Palmowski M, Lederle W, Woenne EC, Hengerer A, Taupitz M, Semmler W, Kiessling F. Assessment of vascular remodeling under antiangiogenic therapy using DCE-MRI and vessel size imaging. J Magn Reson Imaging 2009;29(5):1125-1133.

19. Varallyay CG, Muldoon LL, Gahramanov S, Wu YJ, Goodman JA, Li X, Pike MM, Neuwelt EA. Dynamic MRI using iron oxide nanoparticles to assess early vascular effects of antiangiogenic versus corticosteroid treatment in a glioma model. J Cereb Blood Flow Metab 2009;29(4):853-860.

20. Batchelor TT, Sorensen AG, di Tomaso E, Zhang W-T, Duda DG, Cohen KS, Kozak KR, Cahill DP, Chen P-J, Zhu M, Ancukiewicz M, Mrugala MM, Plotkin S, Drappatz J, Louis DN, Ivy P, Scadden DT, Benner T, Loeffler JS, Wen PY, Jain RK. AZD2171, a pan-VEGF receptor tyrosine kinase inhibitor, normalizes tumor vasculature and alleviates edema in glioblastoma patients. Cancer Cell 2007;11(1):83-95.

21. Wilhelm S, Carter C, Lynch M, Lowinger T, Dumas J, Smith RA, Schwartz B, Simantov R, Kelley S. Discovery and development of sorafenib: a multikinase inhibitor for treating cancer. Nat Rev Drug Discov 2006;5(10):835-844.

22. Yang F, Van Meter TE, Buettner R, Hedvat M, Liang W, Kowolik CM, Mepani N, Mirosevich J, Nam S, Chen MY, Tye G, Kirschbaum M, Jove R. Sorafenib inhibits signal transducer and activator of transcription 3 signaling associated with growth arrest and apoptosis of medulloblastomas. Mol Cancer Ther 2008;7(11):3519-3526.

23. Siegelin MD, Raskett CM, Gilbert CA, Ross AH, Altieri DC. Sorafenib exerts anti-glioma activity in vitro and in vivo. Neurosci Lett 2010.

24. Jacquier A, Wendland M, Do L, Robert P, Corot C, Higgins CB, Saeed M. MR imaging assessment of the kinetics of P846, a new gadolinium-based MR contrast medium, in ischemically injured myocardium. Contrast Media Mol Imaging 2008;3(3):112-119.

25. Redgate ES, Deutsch M, Boggs SS. Time of death of CNS tumor-bearing rats can be reliably predicted by body weight-loss patterns. Lab Anim Sci 1991;41(3):269-273.

26. Valable S, Lemasson B, Farion R, Beaumont M, Segebarth C, Remy C, Barbier EL. Assessment of blood volume, vessel size, and the expression of angiogenic factors in two rat glioma models: a longitudinal in vivo and ex vivo study. NMR Biomed 2008;21(10):1043-1056.

27. Koh D-M, Collins DJ. Diffusion-weighted MRI in the body: applications and challenges in oncology. AJR Am J Roentgenol 2007;188(6):1622-1635.

28. Mancuso MR, Davis R, Norberg SM, O'Brien S, Sennino B, Nakahara T, Yao VJ, Inai T, Brooks P, Freimark B, Shalinsky DR, Hu-Lowe DD, McDonald DM. Rapid vascular regrowth in tumors after reversal of VEGF inhibition. J Clin Invest 2006;116(10):2610-2621.

29. Inai T, Mancuso M, Hashizume H, Baffert F, Haskell A, Baluk P, Hu-Lowe DD, Shalinsky DR, Thurston G, Yancopoulos GD, McDonald DM. Inhibition of vascular endothelial growth factor (VEGF) signaling in cancer causes loss of endothelial fenestrations, regression of tumor vessels, and appearance of basement membrane ghosts. Am J Pathol 2004;165(1):35-52.

30. Turetschek K, Preda A, Novikov V, Brasch RC, Weinmann HJ, Wunderbaldinger P, Roberts TPL. Tumor microvascular changes in antiangiogenic treatment: assessment by magnetic resonance contrast media of different molecular weights. J Magn Reson Imaging 2004;20(1):138-144.

31. Jain RK. Normalization of tumor vasculature: an emerging concept in antiangiogenic therapy. Science 2005;307(5706):58-62.

32. Nakamura K, Taguchi E, Miura T, Yamamoto A, Takahashi K, Bichat F, Guilbaud N, Hasegawa K, Kubo K, Fujiwara Y, Suzuki R, Shibuya M, Isae T. KRN951, a highly potent inhibitor of vascular endothelial growth factor receptor tyrosine kinases, has antitumor activities and affects functional vascular properties. Cancer Res 2006;66(18):9134-9142.

33. Tofts PS, Berkowitz B, Schnall MD. Quantitative analysis of dynamic Gd-DTPA enhancement in breast tumors using a permeability model. Magn Reson Med 1995;33(4):564-568.

34. Tofts PS, Kermode AG. Measurement of the blood-brain barrier permeability and leakage space using dynamic MR imaging. 1. Fundamental concepts. Magn Reson Med 1991;17(2):357-367.

35. Beaumont M, Lemasson B, Farion R, Segebarth C, Remy C, Barbier EL. Characterization of tumor angiogenesis in rat brain using iron-based vessel

size index MRI in combination with gadolinium-based dynamic contrast-enhanced MRI. J Cereb Blood Flow Metab 2009;29(10):1714-1726.

36. Barbier EL, Lamalle L, Décorps M. Methodology of brain perfusion imaging. J Magn Reson Imaging 2001;13(4):496-520.

37. He X, Yablonskiy DA. Quantitative BOLD: mapping of human cerebral deoxygenated blood volume and oxygen extraction fraction: default state. Magn Reson Med 2007;57(1):115-126.

Table 1

Group	Subgroup	$D13_{(T-1)}$	$D15_{(T1)}$	$D18_{(T4)}$	$D28_{(T14)}$
Untreated	Longitudinal	4	4	4	3
	Single-time	3	3	3	1
	Total	**7**	**7**	**7**	**4**
BCNU	Longitudinal	4	4	3	2
	Single-time	3	3	4	2
	Total	**7**	**7**	**7**	**4**
SORA	Longitudinal	4	4	3	2
	Single-time	3	3	4	2
	Total	**7**	**7**	**7**	**4**

Table 1: Data available for each group (untreated, BCNU and SORA), each subgroup (longitudinal and single-time) and each time point ($D13_{(T-1)}$, $D15_{(T1)}$, $D18_{(T4)}$ and $D28_{(T14)}$).

Legends

Figure 1. a) Experimental protocol. At D0 60 rats were orthotopically implanted with 10^5 U-87 MG glioma cells. Eleven days later (D11) animals were randomized and stratified into 3 groups (n=20 per group) with similar mean tumor volume (using anatomical images). BCNU group received two intravenous injections of BCNU the first and the 13th day after treatment onset ($D14_{(T0)}$ and $D27_{(T13)}$). SORA group received daily oral administration of Sorafenib between the treatment onset and the 14th day after ($D14_{(T0)}$ to $D28_{(T14)}$). Untreated group received no treatment. For each group, 4 rats, called "longitudinal" subgroup were imaged at each time point ($D13_{(T-1)}$, $D15_{(T1)}$, $D18_{(T4)}$ and $D28_{(T14)}$). After the last MRI measurement, animals were euthanized for subsequent *ex vivo* experiments. Per group, the sixteen remaining rats, called "single-time" subgroup, were imaged once and then euthanized at the end of imaging session to enable ex-vivo studies (4 animals/time point). b) Diagram of the MRI experiments for tumor follow-up (the main experiment). c) Diagram of the control MRI experiment designed to evaluate the USPIO extravasations (realized on an additional set of animal).

Figure 2. a) Percent of animal survival as function of time. Open squares show the survival time of untreated rats. Cross and open circles represent the animals treated by BCNU and Sorafenib, respectively. (n = 6 per group). Increased lifespan was presented for BCNU and SORA groups (%). b) Tumor volumes for untreated, BCNU and SORA groups assessed by MRI as function of time. Mean ± SD. p<0.001: ***, untreated versus SORA group; p<0.001: $$$; untreated versus BCNU group. p<0.001: ¥¥¥; SORA versus BCNU group.

Figure 3. *In vivo* MRI estimated parameters. (a) Evolution of ADC, (b) microvessel diameter (VSI), (c) blood volume fraction (BVf) and (d) vessel permeability (CE-MRI) as function of time across each group. A representative map and the averaged value for group analysis are shown for each parameter and for each group at each time point. Dotted lines on MRI maps represent tumor ROI determined from anatomical images. Mean ± SD. $p<0.05$: *, $p<0.01$: **, $p<0.001$: ***, untreated versus SORA group; $p<0.001$: $$$; untreated versus BCNU group.

Figure 4. Ex-vivo study. a) Histological and immunohistological images at $D28_{(T14)}$. Example of hematoxylin/eosine (HE) staining representative of contralateral and intratumoral tissue in the untreated, BCNU and SORA groups. Black arrows point to the hypostained intratumoral edema. Collagen IV and RecA stainings representative of contralateral striatum and of tumor region for each group. White arrows point to intratumoral vessel only stained by collagen IV in SORA group. The cells density (cells/mm^2) and the percentage of vessels doubly stained have been added to the HE and to the merged images respectively. Scale bar = 100 µm. b-c-d) Quantitative analysis of the collagen IV staining. Evolution of (b) vessel diameter, (c) vascular area and (d) vessels density as function of time across each group. MeanSD. *: $P<0.05$; **:$p<0.01$

Figure 1.

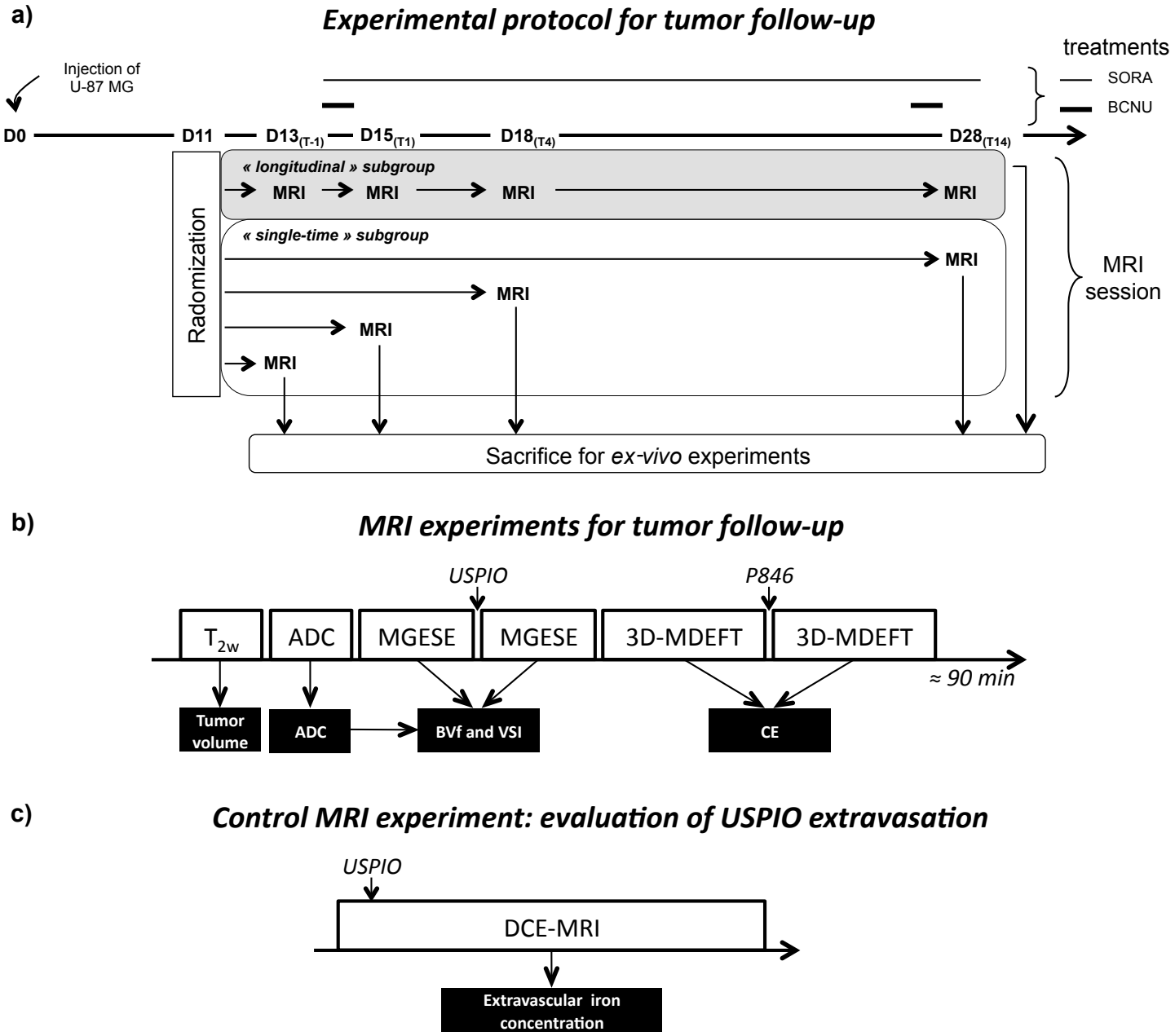
a)
Experimental protocol for tumor follow-up
treatments
SORA
BCNU
Injection of U-87 MG
D0
D11
D13(T-1)
D15(T1)
D18(T4)
D28(T14)
Radomization
« longitudinal » subgroup
MRI
MRI
MRI
MRI
« single-time » subgroup
MRI
MRI
MRI
MRI
MRI session
Sacrifice for ex-vivo experiments
b)
MRI experiments for tumor follow-up
USPIO
P846
T2w
ADC
MGESE
MGESE
3D-MDEFT
3D-MDEFT
≈ 90 min
Tumor volume
ADC
BVf and VSI
CE
c)
Control MRI experiment: evaluation of USPIO extravasation
USPIO
DCE-MRI
Extravascular iron concentration

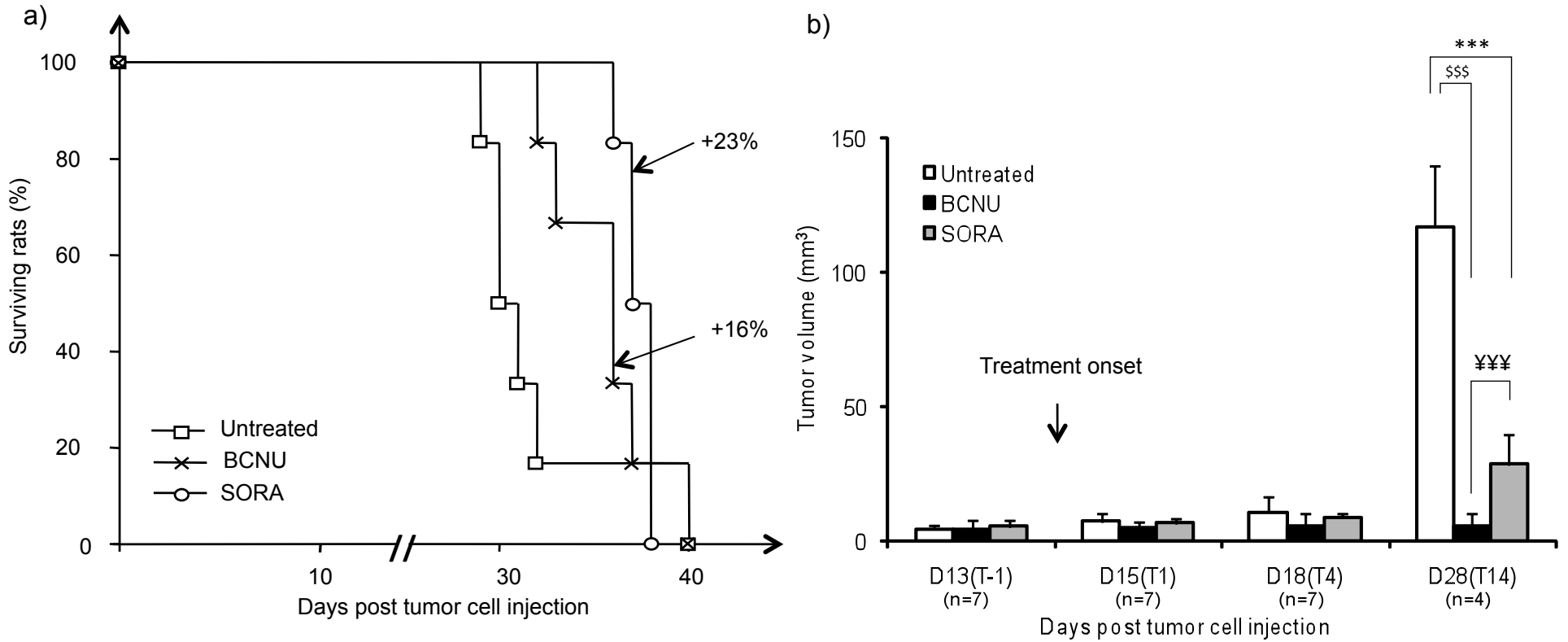
a)
Surviving rats (%)
100
80
60
40
20
0
10
30
40
Days post tumor cell injection
Untreated
BCNU
SORA
+23%
+16%
b)
Tumor volume (mm³)
150
100
50
0
Untreated
BCNU
SORA
Treatment onset
***
$$$
¥¥¥
D13(T-1)
(n=7)
D15(T1)
(n=7)
D18(T4)
(n=7)
D28(T14)
(n=4)
Days post tumor cell injection

Figure 3.

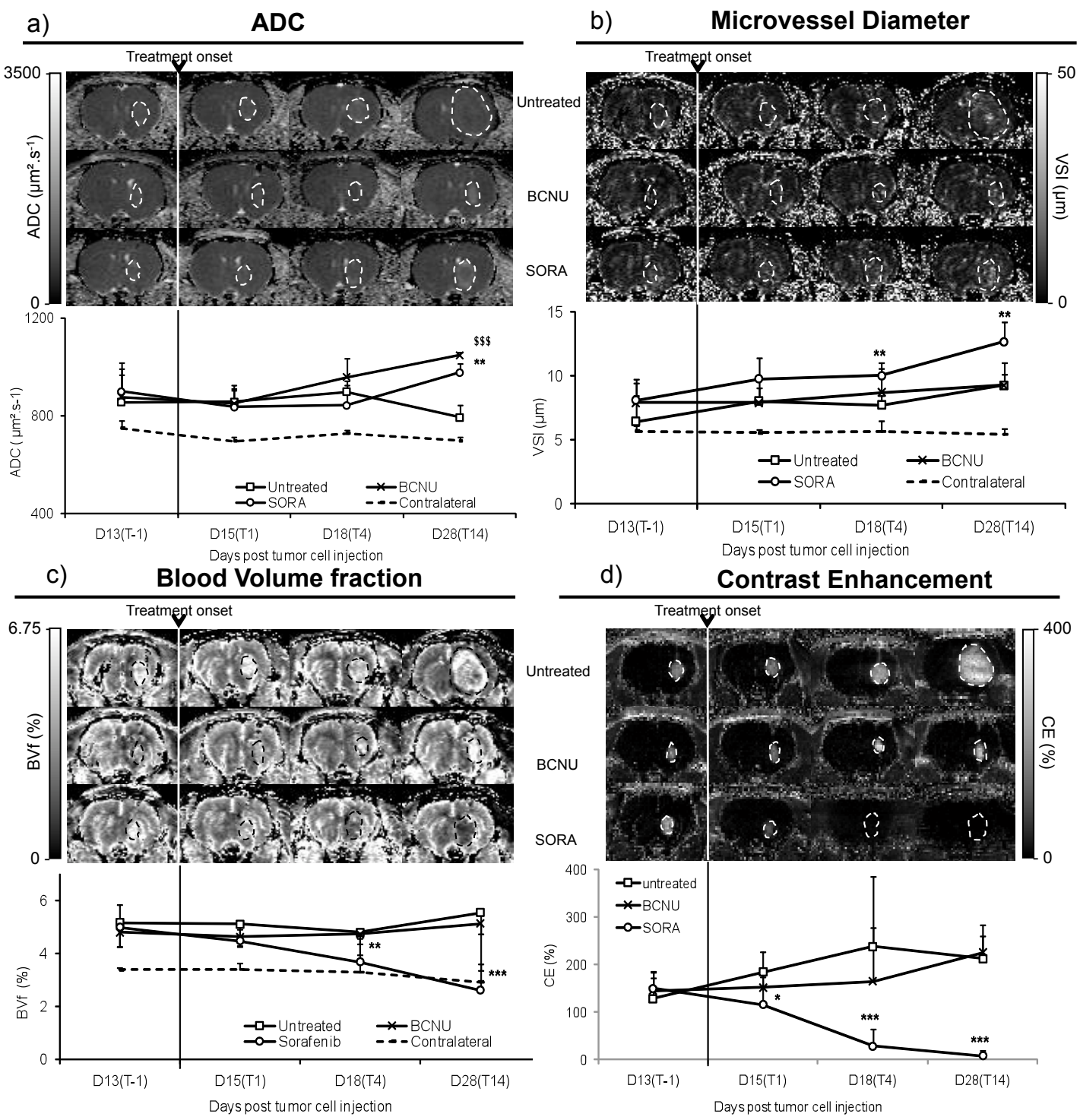
a)
ADC
Treatment onset
3500
0
ADC (µm².s-1)
Untreated
BCNU
SORA
1200
800
400
ADC (µm².s-1)
$$$
**
Untreated
BCNU
SORA
Contralateral
D13(T-1)
D15(T1)
D18(T4)
D28(T14)
Days post tumor cell injection
b)
Microvessel Diameter
Treatment onset
50
0
VSI (µm)
15
10
5
0
VSI (µm)
**
**
Untreated
BCNU
SORA
Contralateral
D13(T-1)
D15(T1)
D18(T4)
D28(T14)
Days post tumor cell injection
c)
Blood Volume fraction
Treatment onset
6.75
0
BVf (%)
6
4
2
0
BVf (%)
**
***
Untreated
BCNU
Sorafenib
Contralateral
D13(T-1)
D15(T1)
D18(T4)
D28(T14)
Days post tumor cell injection
d)
Contrast Enhancement
Treatment onset
400
0
CE (%)
Untreated
BCNU
SORA
400
300
200
100
0
CE (%)
untreated
BCNU
SORA
*
***
***
D13(T-1)
D15(T1)
D18(T4)
D28(T14)
Days post tumor cell injection

Figure 4.

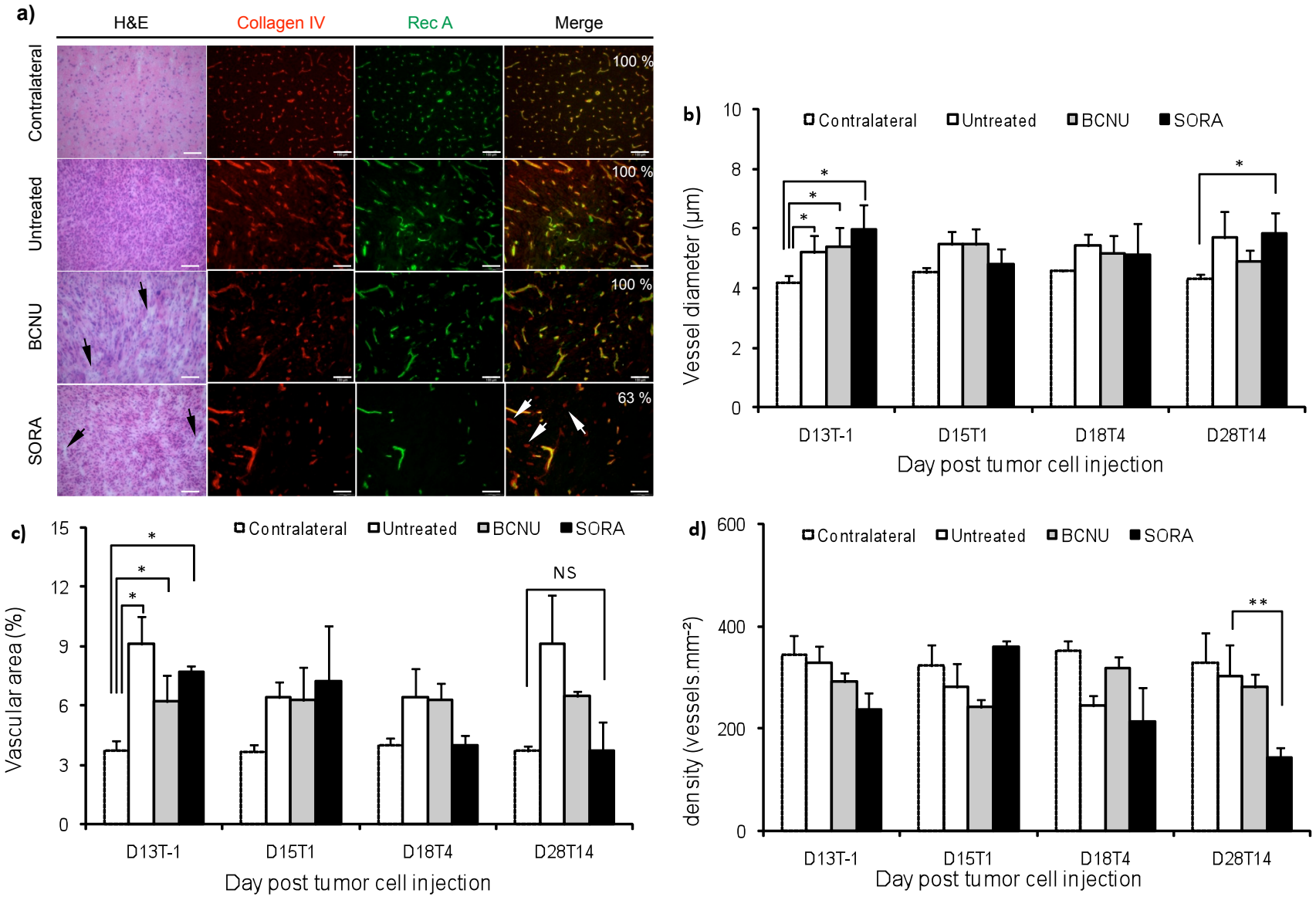
a)
H&E
Collagen IV
Rec A
Merge
Contralateral
Untreated
BCNU
SORA
100 %
100 %
100 %
63 %
b)
Contralateral
Untreated
BCNU
SORA
Vessel diameter (µm)
D13T-1
D15T1
D18T4
D28T14
Day post tumor cell injection
c)
Vascular area (%)
NS
d)
density (vessels.mm-2)
**